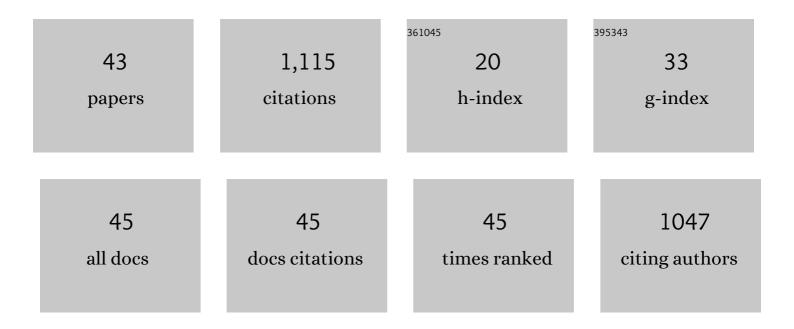
Wojciech J PrzybyÅ,owicz

List of Publications by Year in descending order

Source: https://exaly.com/author-pdf/7667697/publications.pdf Version: 2024-02-01



#	Article	IF	CITATIONS
1	Comparison of essential and nonâ€essential element distribution in leaves of the Cd/Zn hyperaccumulator <i>Thlaspi praecox</i> as revealed by microâ€PIXE. Plant, Cell and Environment, 2008, 31, 1484-1496.	2.8	114
2	Xâ€ray elemental mapping techniques for elucidating the ecophysiology of hyperaccumulator plants. New Phytologist, 2018, 218, 432-452.	3.5	104
3	Spatial distribution of cadmium in leaves of metal hyperaccumulating <i>Thlaspi praecox</i> using microâ€PIXE. New Phytologist, 2008, 179, 712-721.	3.5	91
4	Proton microprobe and X-ray fluorescence investigations of nickel distribution in serpentine flora from South Africa. Nuclear Instruments & Methods in Physics Research B, 1994, 89, 208-212.	0.6	68
5	Iron and ferritin accumulate in separate cellular locations in Phaseolus seeds. BMC Plant Biology, 2010, 10, 26.	1.6	67
6	Micro-PIXE in plant sciences: Present status and perspectives. Nuclear Instruments & Methods in Physics Research B, 2002, 189, 470-481.	0.6	65
7	Heavy metal distribution in Suillus luteus mycorrhizas – as revealed by micro-PIXE analysis. Nuclear Instruments & Methods in Physics Research B, 2001, 181, 649-658.	0.6	46
8	Investigation of Ni hyperaccumulation by true elemental imaging. Nuclear Instruments & Methods in Physics Research B, 1995, 104, 176-181.	0.6	44
9	Quantitative micro-PIXE comparison of elemental distribution in Ni-hyperaccumulating and non-accumulating genotypes of Senecio coronatus. Nuclear Instruments & Methods in Physics Research B, 1997, 130, 368-373.	0.6	38
10	Functional analysis of metals distribution in organs of the beetle Chrysolina pardalina exposed to excess of nickel by Micro-PIXE. Nuclear Instruments & Methods in Physics Research B, 2003, 210, 343-348.	0.6	35
11	X-ray microanalysis of biological material in the frozen-hydrated state by PIXE. Microscopy Research and Technique, 2007, 70, 55-68.	1.2	35
12	In-vacuum micro-PIXE analysis of biological specimens in frozen-hydrated state. Nuclear Instruments & Methods in Physics Research B, 2007, 260, 141-148.	0.6	33
13	Zinc-induced DNA damage and the distribution of metals in the brain of grasshoppers by the comet assay and micro-PIXE. Comparative Biochemistry and Physiology Part - C: Toxicology and Pharmacology, 2006, 144, 242-251.	1.3	32
14	Freeze-substitution methods for Ni localization and quantitative analysis in Berkheya coddii leaves by means of PIXE. Nuclear Instruments & Methods in Physics Research B, 2005, 231, 338-344.	0.6	28
15	Micro-PIXE studies of elemental distribution in seeds of Silene vulgaris from a zinc dump in Olkusz, southern Poland. Nuclear Instruments & Methods in Physics Research B, 1999, 158, 306-311.	0.6	23
16	Elemental distribution in lichens transplanted to polluted forest sites near Kraków (Poland). Nuclear Instruments & Methods in Physics Research B, 2002, 189, 499-505.	0.6	23
17	Elemental microanalysis in ecophysiology using ion microbeam. Nuclear Instruments & Methods in Physics Research B, 2004, 219-220, 57-66.	0.6	23
18	Elemental distribution and chemical speciation of copper and cobalt in three metallophytes from the copper–cobalt belt in Northern Zambia. Metallomics, 2020, 12, 682-701.	1.0	23

#	Article	IF	CITATIONS
19	Tools for the Discovery of Hyperaccumulator Plant Species and Understanding Their Ecophysiology. Mineral Resource Reviews, 2018, , 117-133.	1.5	21
20	Nuclear microprobe studies of elemental distribution in seeds of Biscutella laevigata L. from zinc wastes in Olkusz, Poland. Nuclear Instruments & Methods in Physics Research B, 2001, 181, 634-639.	0.6	20
21	True elemental imaging of pyrites from Witwatersrand reefs. Nuclear Instruments & Methods in Physics Research B, 1995, 104, 450-455.	0.6	18
22	Nuclear microprobe studies of elemental distributions in dormant seeds of Burkea africana. Nuclear Instruments & Methods in Physics Research B, 1997, 130, 381-387.	0.6	18
23	Abnormal concentrations of Cu–Co in <i>Haumaniastrum katangense</i> , <i>Haumaniastrum robertii</i> and <i>Aeolanthus biformifolius</i> : contamination or hyperaccumulation?. Metallomics, 2019, 11, 586-596.	1.0	17
24	Micro-PIXE investigation of bean seeds to assist micronutrient biofortification. Nuclear Instruments & Methods in Physics Research B, 2011, 269, 2297-2302.	0.6	12
25	X-ray fluorescence elemental mapping of roots, stems and leaves of the nickel hyperaccumulators Rinorea cf. bengalensis and Rinorea cf. javanica (Violaceae) from Sabah (Malaysia), Borneo. Plant and Soil, 2020, 448, 15-36.	1.8	11
26	Micro-PIXE analysis: importance of biological sample preparation techniques. Radiation Physics and Chemistry, 2004, 71, 785-786.	1.4	10
27	Quantitative mapping of elemental distribution in leaves of the metallophytes Helichrysum candolleanum, Blepharis aspera, and Blepharis diversispina from Selkirk Cu–Ni mine, Botswana. Nuclear Instruments & Methods in Physics Research B, 2015, 363, 188-193.	0.6	10
28	Endosperm prevents toxic amounts of Zn from accumulating in the seed embryo – an adaptation to metalliferous sites in metal-tolerant <i>Biscutella laevigata</i> . Metallomics, 2020, 12, 42-53.	1.0	9
29	Environmental pollution monitoring using lichens as bioindicators: a micro-PIXE study. Radiation Physics and Chemistry, 2004, 71, 783-784.	1.4	8
30	Mycorrhizal fungi modify element distribution in gametophytes and sporophytes of a fern Pellaea viridis from metaliferous soils. Chemosphere, 2013, 92, 1267-1273.	4.2	8
31	Elemental distribution patterns in the skins of false killer whales (Pseudorca crassidens) from a mass stranding in South Africa, analysed using micro-PIXE. Nuclear Instruments & Methods in Physics Research B, 2015, 363, 70-74.	0.6	7
32	Mineralizing fluids of the supergene-enriched Mashitu South Cu-Co deposit, Katanga Copperbelt, DRC. Ore Geology Reviews, 2019, 109, 201-228.	1.1	7
33	Co-Localization of Copper, Zinc and Lead with Calcium in Their Accumulation Sites in the Housefly's Abdomen by Micro-PIXE. Mikrochimica Acta, 2006, 155, 301-304.	2.5	6
34	Stopping power of Nd, Pm and Sm ions in Cd determined with -ray lineshape analysis. Nuclear Instruments and Methods in Physics Research, Section A: Accelerators, Spectrometers, Detectors and Associated Equipment, 2009, 607, 591-599.	0.7	6
35	Zinc allocation to and within <i>Arabidopsis halleri</i> seeds: Different strategies of metal homeostasis in accessions under divergent selection pressure. Plant-Environment Interactions, 2020, 1, 207-220.	0.7	5
36	Ecophysiology of nickel hyperaccumulating plants from South Africa – from ultramafic soil and mycorrhiza to plants and insects. Metallomics, 2020, 12, 1018-1035.	1.0	5

#	Article	IF	CITATIONS
37	Multimodal synchrotron X-ray fluorescence imaging reveals elemental distribution in seeds and seedlings of the Zn–Cd–Ni hyperaccumulator <i>Noccaea caerulescens</i> . Metallomics, 2022, 14, .	1.0	5
38	Methods for Visualizing Elemental Distribution in Hyperaccumulator Plants. Mineral Resource Reviews, 2021, , 197-214.	1.5	4
39	Micro-PIXE characterisation of uranium occurrence in the coal zones and the mudstones of the Springbok Flats Basin, South Africa. Nuclear Instruments & Methods in Physics Research B, 2017, 404, 114-120.	0.6	3
40	Convergent patterns of tissue-level distribution of elements in different tropical woody nickel hyperaccumulator species from Borneo Island. AoB PLANTS, 2020, 12, plaa058.	1.2	3
41	Aspects of Chemical Composition of Exodermal Cell Walls in Roots of Ni-Hyperaccumulating and Non-Hyperaccumulating Genotypes of Senecio coronatus. Microscopy and Microanalysis, 2014, 20, 1276-1277.	0.2	1
42	Geological Studies by Means of Proton Microbeam System. Acta Physica Polonica A, 2001, 100, 679-686.	0.2	0
43	Contrasting patterns of nickel distribution in the hyperaccumulators <i>Phyllanthus balgooyi</i> and <i>Phyllanthus rufuschaneyi</i> from Malaysian Borneo. Metallomics, 2022, 14, .	1.0	Ο